FIRE AND MATERIALS, VOL. 16, 197-206 {1992)

Burning Rate of Solid Wood Measured in a Heat Release Rate Calorimeter

Hao C. Tran and Robert H. White
USDA Forest Service, Forest Products Laboratory. One Gifford Pinchot Drive, Madison, WI 53705-2398, USA

Burning rate is a key factor in modeling fire growth and fire endurance of wood structures. This study investigated the burning rate of selected wood materials as determined by heat release, mass loss and charring rates. Thick samples of redwood, southern pine, red oak and basswood were tested in a heat release rate calorimeter. Results on ignitability and average beat release, mass loss and charring rates are reported for a heat flux range between 15 and 55 kW m $^{-2}$. In this range, burning rate increased linearly with heat flux. Burning rate was very species dependent. Heat release rate was related to mass loss by effective heat of combustion, which also increased with beat flux. Charring rate was related to mass loss rate and original wood density. Important char property data such as yield, density and contraction are reported. A simplified calculation method is proposed for calculating mass loss rate and charring rate based on heat release rate.

INTRODUCTION

Burning rate is a general term used to describe the rate at which a given material is consumed by fire. Specifically, burning rate can be described in terms of heat release rate, mass loss rate or, in the case of charring materials, charring rate. All of these are related because wood is a charring material. Some relationships between these aspects of burning rate have been determined experimentally and by theoretical modeling methods.

The concept of heat release rate has spurred development of numerous measuring devices. Only some published data on wood are mentioned here. Brenden[1] used an apparatus based on heat and mass balance but it never became popular. Chamberlain[2] reviewed heat release calorimeters and published heat release data of some wood-based products using various National Bureau of Standards (NBS) calorimeters. (The NBS is now called the National Institute of Standards and Technology (NIST).) More recently, Tran[3] documented heat release rate data of various wood materials tested in the Cone Calorimeter at NIST and a modified Ohio State University (OSU) apparatus at the Forest Products Laboratory (FPL).

In predicting fire resistance of wood members, analysis is based on reduction of the member cross-section as a result of charring. White[6,7] established an empirical model of charring rate as a function of density, moisture content, transport properties and chemical composition. The experiments were carried out under ASTM E 119 conditions simulating a fully developed fire. Although there are charring data for other time–temperature curves,[9,10] data for specific heat fluxes are limited.

Mikkola[11] presented some experimental charring rate data for wood using the Cone Calorimeter and described a simplified model to calculate charring rate based on density, moisture content, external heat flux and oxygen concentration of the surrounding air. Parker[12] developed a theoretical heat transfer model to calculate both heat release rate and charring rate. Although reasonable agreement with some experimental data was achieved, both models need validation with a more extensive database,

This report presents the initial phase of our study with the following objectives:

(1) To establish a database of ignition data and heat release, charring, and mass loss rates of some common wood species as a function of time and external heat flux;
(2) To derive a simplified and practical approach to relate heat release, charring and mass loss rates for wood materials.

METHODS AND MATERIALS

Current test methods are designed to evaluate materials in the simplest arrangement possible. Because fire is so complex, efforts to mimic 'real' fire with bench-scale testing are almost futile. Instead, the predominant philosophy of fire testing is to simply quantify the 'reaction to fire' given fixed conditions. These quantities can then be used in calculation procedures that keep track of the changing conditions in fire. The conditions that are normally controlled in fire tests are radiant heat flux (the dominant mode of heat transfer in fire) and ignition mode.

At the USDA Forest Service, Forest Products Laboratory (FPL), we have used an OSU apparatus to quantify heat and smoke release rate from wood products at different heat flux levels. The OSU apparatus has been modified to improve its accuracy and to obtain information that otherwise would not be available. In the study reported here, thick samples from four selected wood species representing a subset of materials used by White[6,7] were exposed to a range of heat fluxes from 15 to 55 kW m^{-2}. Ignition time and heat release, charring and mass loss rates were obtained from each test.

Modified OSU apparatus

The OSU apparatus is a flow-through device in which a square sample is exposed to a electrically powered radiant panel. The combustion products are carried into

Received April 1992
Accepted 1 June 1992

a constant flow of air flowing through the chamber. Heat release rate from the sample is sensed thermally via an array of thermocouples, called a thermopile in ASTM E 906 standard. To improve accuracy, the OSU apparatus was modified in three ways:

(1) Addition of the oxygen-consumption calorimetry technique. The oxygen-consumption method is the state of the art in heat release measurement. This sensing method is accurate and independent of thermal complications of different apparatuses;
(2) Addition of an auxiliary heat flux meter to monitor heat flux during tests;
(3) Gas phase piloted ignition of the sample. The pilot flame is situated above the specimen. When wood is exposed to heat, it pyrolyzes. When the rate of pyrolyzate production is sufficiently high to produce a combustible gas–air mixture, this mixure can be ignited by a flame or spark.

Details of these modifications and the operation of the apparatus were documented by Tran.[13] A mass loss measurement system using the injection shaft as a lever was added to monitor sample mass loss during the test. However, in the analysis, which examined only average data throughout the test, we used mass loss obtained by weighing the sample before and after the test. A general schematic of the equipment is given in Fig. 1.

Materials and test samples

The four species used in this study were a half-fraction of eight species used in previous studies[6,7] and were selected based on a factorial design. The three variables were density (low/high), permeability (low/high) and species type (softwood/hardwood). Permeability was based on depth of penetration of a copper–chrome–arsenate (CCA) solution in a pressure treatment. The four species were redwood *(Sequoia sempervirens)*, southern pine *(Pinus* sp.), red oak *(Quercus* sp.) and basswood *(Tilia* sp.) from the same stock as those used in previous studies.[6,7] In these studies, char formation was found to play an important role in the charring rate of wood. This confirmed similar conclusions based on a theoretical model.[14] The measure of char formation was the char contraction factor (f_c) which is defined as the linear volume fraction of the pyrolyzed wood that is converted to char. The properties measured in these studies are given in Table 1.

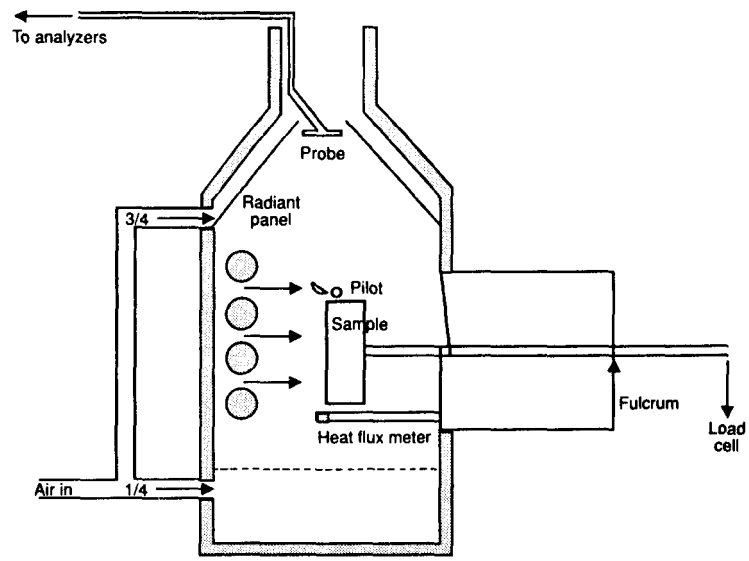

Figure 1. **Schematic diagram of FPL-modified OSU apparatus**

Table 1. Test materials[a]

Species	Type	ρ_w (kg m^{-3})	Moisture (%)	Klason lignin (%)	Penetration (mm)	f_c	$\dot{c}$ (mm min^{-1})
Redwood	Softwood	312	8.33	37.1	4	0.862	0.74
Southern pine	Softwood	508	9.71	27.9	31	0.589	0.77
Red oak	Hardwood	660	8.53	24.5	3	0.703	0.58
Basswood	Hardwood	420	8.06	19.8	30	0.542	0.87

[a] ρ_w was based on weight and volume of oven-dried wood.
Klason lignin content was based on oven-dried, extractive-free wood.
Penetration was based on depth of penetration of CCA in treatability tests, used as indicator of transverse permeability.
f_c and $\dot{c}$ were measured under ASTM E 119 conditions.

A diagram of a typical sample is shown in Fig. 2. The samples were prepared by glueing strips of wood to form 150 mm × 150 mm × 64 mm blocks. The strips were of various thickness, with a minimum of 38 mm. One 150 mm × 150 mm surface was exposed to the radiant flux. Heat flux was perpendicular to the direction of the wood grain, which was horizontal in all tests. The predominant direction of the annual rings was perpendicular to the sample surface. Therefore, the direction of the heat flux was tangential to the annual rings. Six type-K chromel alumel thermocouples with wire thickness of 0.12 mm were imbedded in the samples at depths of 0, 6, 12, 18, 24 and 36 mm from the exposed surface. The surface thermocouple was simply pressed against the wood surface to give some indication of ignition temperature. Measuring surface temperature is very difficult, and no attempt was made to maintain the contact between the thermocouple and the surface during the tests. The other thermocouple leads were parallel to the exposed surface to minimize conduction error. All samples were conditioned at 23°C and 50% relative humidity, resulting in an average moisture content of 8–9%.

Fire tests

The samples were mounted in the holder designed for the OSU apparatus. The unexposed sides were wrapped in aluminum foil to minimize mass loss and to approach a one-dimensional case. No insulation backing was used because the sample thickness occupied the whole depth of the holder (65 mm). Data acquisition was set at 15-s sampling intervals. Following a baseline of 2.5 min, the sample was injected into the chamber. Ignition time, the time from injection to ignition of the sample, was obtained with a stopwatch. Tests were terminated when the thermocouple at 36-mm depth recorded 300°C.

Four nominal flux levels were selected: 15, 25, 35 and 50 kW m^{-2}. The flux levels are called nominal because they were not constant during the tests, as is explained in the Results. Thus, the series of tests included four species, four flux levels, and two replicates of each, resulting in a total of 32 tests.

RESULTS

Several types of results were obtained from each test: a history curve of incident radiant flux, ignition time, heat release rate curve as calculated by oxygen consumption method, and mass loss.

Flux history curve

The radiant flux to the sample was generated by a steadily powered radiant panel. It was generally assumed that the flux to the sample was constant and equal to the flux calibrated prior to the tests. In fact, this assumption was not correct. When the sample was injected, the flux decreased slightly from the baseline value. After ignition, the heat generated from the flame caused an increase in temperature of the heating environment and reradiated back to the sample, resulting in an increase in actual incident flux. Examples of flux history of several tests with basswood are shown in Fig. 3. Because of the unique heat flux history for each sample, the average heat flux from ignition to the end of each test was used in data analysis instead of the nominal heat flux levels.

Ignition time

Ignition times of the samples and the corresponding heat fluxes during the period from injection to ignition are given in Table 2. As shown in the table, ignition time is some inverse function of flux. This is intuitive; the faster the wood is heated, the sooner it ignites.

Piloted ignition has been the subject of many theoretical studies. For wood, ignition time is controlled by thermal properties, in particular, thermal inertia *kpc*. A procedure to derive material properties based on ignition data was proposed by Quintiere and Harkleroad[15] and later refined by Janssens.[16] The Janssens procedure

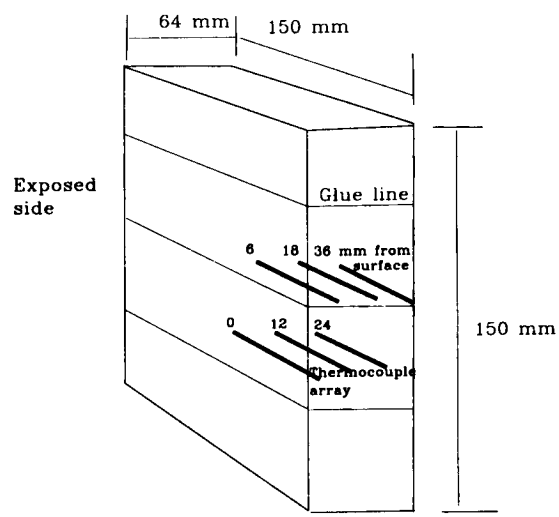

Figure 2. **Typical test sample**

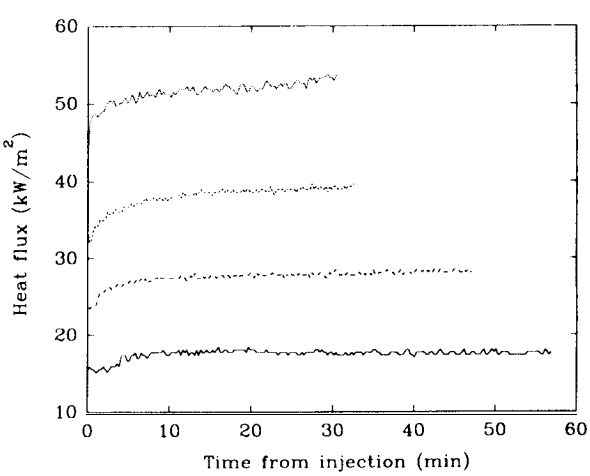

Figure 3. **Typical flux history curves of tests with basswood.**

is used here, The Janssens equation that governs ignition is

$$\dot{q}''_e/\dot{q}''_{cr} = 1 + 0.73\left[\frac{k\rho c}{h_{ig}^2 t_{ig}}\right]^{0.547} \quad (1)$$

where

$\dot{q}''_e$ is external heat flux (kW m^{-2}),
$\dot{q}''_{cr}$ critical heat flux for ignition (kW m^{-2}),
k thermal conductivity (W m^{-1} K^{-1}),
ρ density (kg m^{-3}),
c heat capacity (kJ kg^{-1} K^{-1})
h_{ig} heat transfer coefficient at ignition (W m^{-2} K^{-1}), and
t_{ig} ignition time (s).

A dimensionless form of Eqn (1) is

$$\varphi = 1 + 0.73(1/\tau_{ig})^{0.547} \quad (2)$$

where the terms correspond with the dimensionless groups in Eqn (l).

According to Eqn (1), t_{ig} raised to the power of – 0.547 is a linear function of $\dot{q}''_e$ as shown in Fig. 4 for the four species. Ignition data for flux levels of 50 k W m^{-2} were left out because ignition times were very short (3 -15 s) and a small error in measurement could be significant. Using linear regression, we found values of $\dot{q}''_{cr}$ for the four materials and the slopes of the regression lines. The $\dot{q}''_{cr}$ values are the intercepts between the regression lines and the horizontal axis. The derived data are listed in Table 3.

The *kpc* value of a material can be derived from the slope of the regression line. First, the heat transfer coefficient at ignition h_{ig} is needed to solve Eqn (1), as follows:

$$h_{ig} = \frac{\varepsilon \dot{q}''_{cr}}{(T_{ig} - T_\infty)} \quad (3)$$

Table 2. Ignition times and heat fluxes for various species

Redwood		Southern pine		Red oak		Basswood	
Flux (kW m^{-2})	t_{ig} (s)	Flux (kW m^{-2})	t_{ig} (s)	Flux (kW m^{-2})	t_{ig} (s)	Flux (kW m^{-2})	t_{ig} (s)
16	720	15	909	16	930	15	200
16	762	15	570	16	930	15	165
23	50	22	85	23	120	24	60
23	45	24	85	23	115	22	60
35	16	34	35	34	50	35	12
35	16	34	26	34	50	33	20
46	3	51	5	49	15	46	5
50	3	51	5	50	10	49	5

where

ε is emissivity of the material (assume 0.88 as suggested by Janssens),
T_{ig} surface temperature at ignition (K), and
T_∞ ambient temperature (293 K).

Surface ignition temperature is a very elusive quantity and difficult to measure accurately. For this particular study, it is taken as the average value of the surface thermocouple readings of several tests just prior to ignition. Using T_{ig} the values of h_{ig} were calculated. By this calculation, h_{ig} was found to be fairly constant for different species and an average of 31 W m^{-2} K^{-1} could be assumed. The 'apparent' *kpc* of the materials can be calculated using the following equation:

$$k\rho c = h_{ig}^2 (0.73 \text{ slope } \dot{q}''_{cr})^{-1.8281} \quad (4)$$

Note that the apparent *kpc is* a theoretical value that represents some estimate of thermal inertia of wood heated to a temperature somewhere between ambient and ignition temperature. The *kpc* at ambient temperature was calculated using empirical equations given in the *Wood Handbook.*[17] We found that this value was higher than calculated *kpc* values for ambient temperature (Table 3) by a factor ranging from 1.6 to 2.0. Therefore, an average value of 1.8 was chosen for the following comparison with Janssens' model.

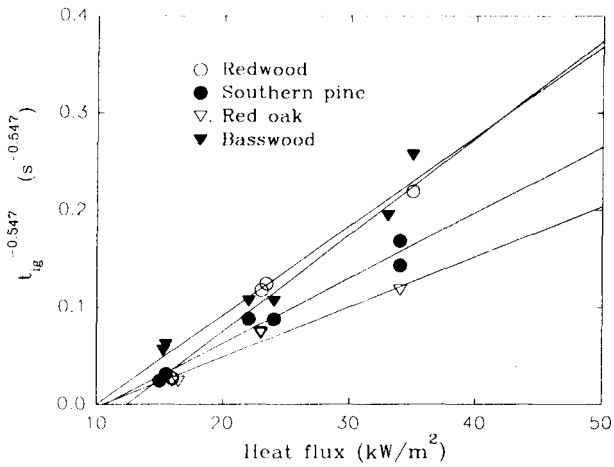

Figure 4. *Piloted ignition data for test species.*

Table 3. Ignition properties of materials[a]

Species	$\dot{q}''_{cr}$ (kW m^{-2})	Slope	T_{ig} (°C)	h_{ig} (W m^{-2} K^{-1})	$k\rho c$ (kJ^2 K^{-2} m^{-4} s^{-1}) Apparent	$k\rho c$ (kJ^2 K^{-2} m^{-4} s^{-1}) Ambient
Redwood	12.42	0.00996	363	29.9	0.073	0.045
Southern pine	10.68	0.00735	320	31.3	0.183	0.110
Red oak	10.53	0.00516	315	31.4	0.360	0.178
Basswood	10.00	0.00920	298	31.8	0.141	0.077

[a] Terms are defined in the text (see Eqn (1)).
T_{ig} is surface temperature at ignition.

Janssens found that ignition data of different wood materials obtained in the Cone Calorimeter and the LIFT apparatus can be compressed to fit the dimensionless form (Eqn (2)). In Fig. 5 the normalized ignition data for the four materials seem to fit the model quite well. The t_{ig} values were calculated using data from Table 3 with h_{ig} of 31 W m^{-2}K^{-1} for all materials and *kpc* at ambient temperature multiplied by a factor of 1.8. Therefore, good prediction of ignition time at a certain heat flux can be made using this procedure based on literature values of *kpc* at ambient temperature. Janssens found that for the Cone Calorimeter ignition data, his is about 35 W m^{-2}K^{-1} and apparent *kpc is* 2.3 to 2.6 times the value at ambient temperature. Therefore, the procedure works for both apparatuses although the data used to fit the model are apparatus dependent.

Burning rates

In this section, the results are presented in terms of heat release rate (HRR), mass loss rate per unit area $(\dot{m}'')$ and charring rate $(\dot{c})$.

Upon ignition, wood undergoes flaming combustion and releases heat. The HRR is the measure of energy released per unit time (power) per unit area commonly expressed in kilowatts per square meter. Note that the HRR measurement obtained by the oxygen-consumption method is the net heat release; it does not account for the condensation of water produced from burning fuel. The HRR curves of red oak at different flux levels are shown in Fig. 6 as an example. Each curve represents average data of the duplicates. There is a general pattern in all HRR curves. Following ignition, a peak HRR occurs, followed by a more or less exponential decay and an almost steady-state period to the end of the tests. Except for redwood, which had a very short decay period, the other materials reached a steady level in about 10 min.

The shape of the HRR curves always presents a problem as to what kind of data to report. The data reported in the literature include peak HRR and average HRR. The problem with peak HRR is that it is a single value that can be missed as a result of the discrete data sampling interval of many seconds. The error can be large since this peak occurs in steep regions of the curves (see Fig. 6). Average HRR is computed over a fixed period, such as 1, 3, 5 or 10 min. These values represent some average over the time span of interest. However, the time is difficult to standardize.

The depth of the char front has been correlated with temperatures between 280°C and 350°C. For all practical purposes, the difference in char depth across this range of temperature is small because temperature rise is fairly steep in this region. A typical temperature profile history of a test with basswood with a 38 kW m^{-2} heat flux is given in Fig. 7 as an example. As shown in Fig. 7, the surface thermocouple reading rose quickly because basswood ignited fairly quickly at this flux level. The surface thermocouple then became separated from the surface and read the temperature somewhere in the flame. The rate of rise of the imbedded thermocouple readings decreased with depth as a result of mechanisms of heat and moisture transfer toward the interior of the wood specimen. Therefore, one would expect that the correlation between a temperature such as 300°C and the char front to be better near the exposed surface and not as good

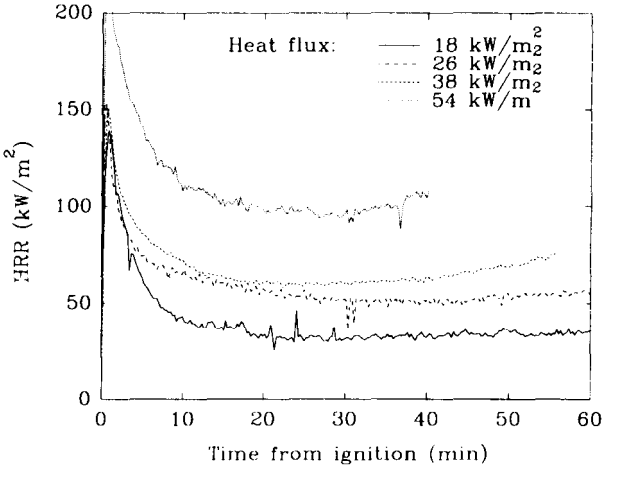

Figure 6. **Rate of heat release (HRR) of red oak.**

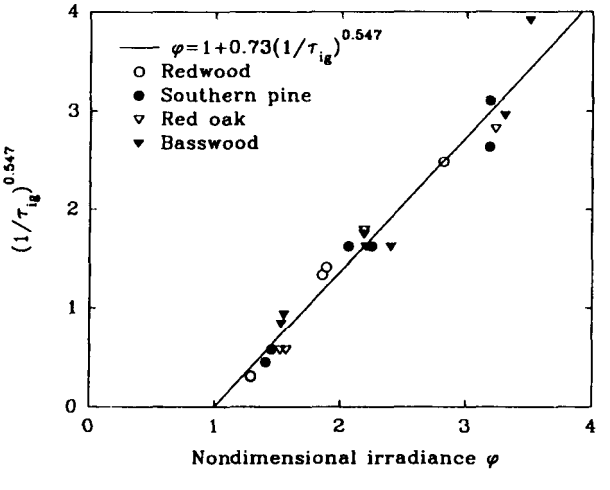

Figure 5. **Correlation of ignition data with Janssens' model.**

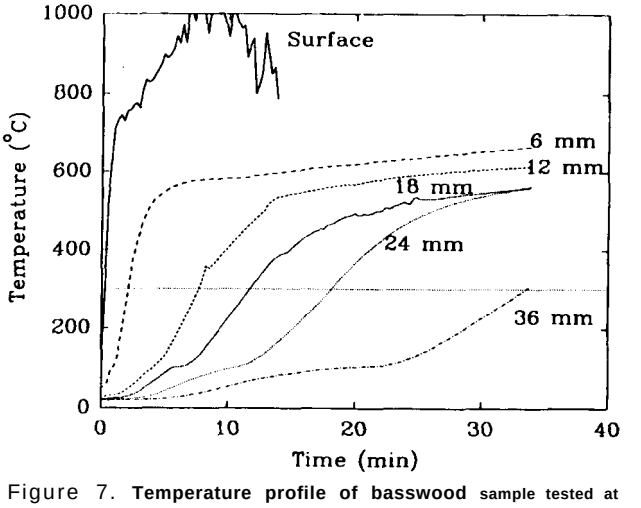

Figure 7. **Temperature profile of basswood sample tested at 38 kW m^{-2} heat flux showing depth of char front (mm).**

with increasing depth. For lack of any exact correlation between temperature and the char front, we decided that 300°C was to be used to indicate the arrival of the char front.

Average charring rate $\dot{c}$ was calculated as 36 mm divided by t_{test}. Table 4 lists the average data of all tests over the test duration from injection to char depth of 36 mm, average values of heat flux, H RR taken from ignition to end of test, mass loss rate per unit area ($\dot{m}''$), charring rate ($\dot{c}$), effective heat of combustion (H_c) and calculated H_c on a dry mass loss basis. The average HRR, $\dot{c}$ and $\dot{m}''$ values are plotted against flux levels in Figs 8, 9 and 10. respectively. As shown, all three measurements are fairly linear functions of flux.

Note that the apparent H_c values are based on average HRR and $\dot{m}''$, which include the moisture driven out of the wood. The H_c can then be adjusted to find the H_c consumed for the dry mass of wood:

$$H_{c,dry} = H_c \left(\frac{\dot{m}''}{\dot{m}''_{dry}} \right) \quad (5)$$

One major problem is the determination of dry mass loss rate. As heat penetrated into the wood slab, moisture was driven in two ways. Some moisture evaporated into the escaping pyrolyzates and some was driven further into the wood and recondensed.[18] To get effective $H_{C,dry}$ over the entire test, Eqn (5) was modified to use total mass loss and calculated total mass loss on a dry basis. Comparison of sample residual weights taken immediately after the test and the weights taken after the samples had been quenched and conditioned showed that the conditioned samples gained about 6% weight.

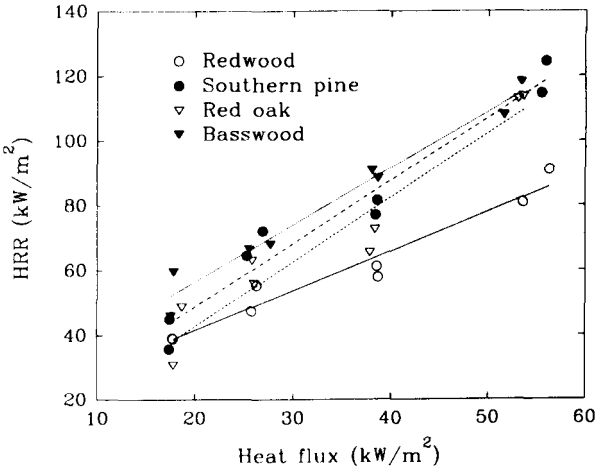

Figure 8. Average HRR as a function of heat flux.

Table 4. Overall data of burning rates

Species	Flux (kW m^{-2})	t_{test} (min)	HRR (kW m^{-2})	$\dot{m}''$ (g m^{-2} s)	$\dot{c}$ (mm min^{-1})	H_c (MJ kg^{-1}) Apparent	Dry basis
Redwood	17.8	66.34	39.0	2.92	0.543	10.93	13.22
	17.7	58.08	39.2	2.92	0.620	10.49	12.88
	25.8	46.66	47.4	3.92	0.771	11.89	14.55
	26.2	55.40	55.3	4.14	0.650	13.19	15.65
	38.5	45.93	61.2	4.75	0.784	12.82	15.17
	38.7	45.20	57.9	4.76	0.800	10.66	12.66
	53.6	37.66	80.9	5.83	0.956	13.86	16.17
	56.3	37.91	90.9	6.25	0.950	14.55	17.07
Southern pine	17.4	95.50	45.0	3.80	0.377	9.97	11.69
	17.4	73.14	35.8	3.77	0.492	8.26	10.14
	25.2	67.31	64.5	4.94	0.535	12.77	14.97
	26.9	52.24	72.1	5.83	0.689	12.03	14.67
	38.5	47.87	77.0	6.74	0.752	11.29	13.47
	38.6	54.92	81.6	6.72	0.655	12.04	14.03
	55.5	42.28	114.7	8.22	0.851	13.95	16.26
	56.0	46.90	124.4	8.99	0.768	13.83	15.82
Red oak	17.8	98.17	—	3.92	0.367	—	—
	18.7	78.49	48.7	4.34	0.460	9.00	11.25
	25.0	66.83	55.8	5.39	0.539	10.05	12.38
	25.8	72.41	63.1	5.81	0.497	10.57	12.57
	37.8	61.48	65.4	6.57	0.586	9.24	11.14
	38.4	57.35	72.6	7.19	0.628	9.95	11.97
	53.1	40.82	112.9	9.80	0.882	11.44	13.93
	53.6	53.22	113.7	9.50	0.676	11.92	13.83
Basswood	17.6	56.86	46.0	4.30	0.633	10.07	12.33
	17.8	50.30	59.6	4.78	0.716	11.77	14.35
	27.7	47.14	67.9	6.21	0.764	10.71	12.74
	25.5	45.68	66.6	6.22	0.788	10.52	12.55
	38.1	32.56	90.8	8.22	1.106	10.93	13.16
	38.7	33.78	88.3	7.66	1.066	11.45	13.70
	51.6	30.62	107.9	9.09	1.176	11.84	14.04
	53.4	32.08	118.1	9.46	1.122	12.46	14.62

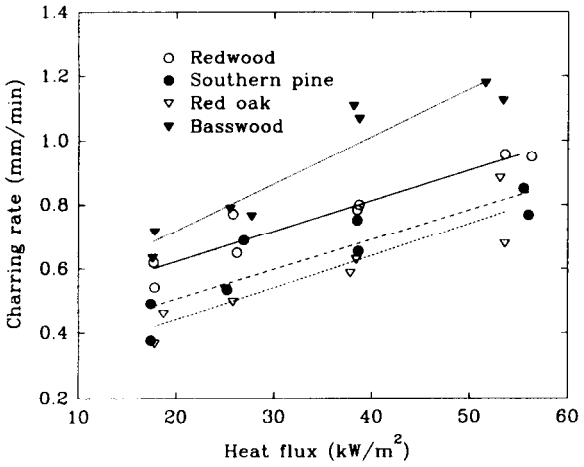

Figure 9. Average charring rate ($\dot{c}$) as a function of heat flux.

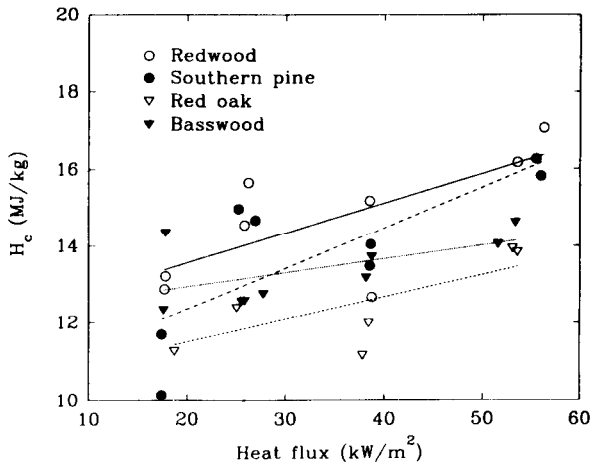

Figure 11. Effective heat of combustion (H_c) on dry basis.

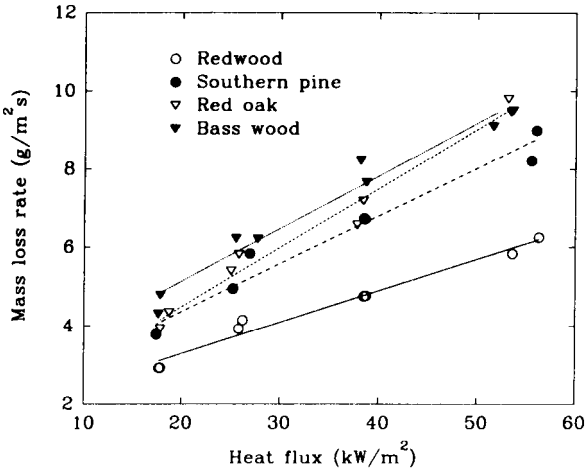

Figure 10. Average mass loss rate ($\dot{m}''$) as a function of heat flux.

Considering that the char weight was about 25% of the residue that did not pick up a significant amount of water, the wood residue was most likely to be free of water at the end of the tests. Thus, using the assumption that the wood residue was moisture-free, the dry mass loss was calculated as follows:

$$m_{\mathrm{dry}} = m_{\mathrm{o}} - m_{\mathrm{H_2O}} - m_{\mathrm{residue}} \tag{6}$$

Equation (5) then becomes

$$H_{\mathrm{c,dry}} = H_{\mathrm{c}}\left(\frac{m}{m_{\mathrm{dry}}}\right) \tag{7}$$

The $H_{\mathrm{c,dry}}$ values are shown in Fig. 11. The $H_{\mathrm{c,dry}}$ measurement is useful as a reference for calculating H_{c} at different moisture levels. As shown in Fig. 11, $H_{\mathrm{c,dry}}$ increased with heat flux. However, the scatter of the data for each species is high.

Char properties

The burned samples were quenched, conditioned at 23°C and 50% RH and then measured for other properties. Weight and thickness of the samples were measured with and without the char. Thicknesses varied significantly within each charred sample. Therefore, measurements were taken as average values of five points, the center and the four quadrant centers of each piece. From the weight and thickness information, we calculated the char contraction factor, char yield and char density.

The char contraction factor is defined as

$$f_{\mathrm{c}} = \frac{X_{\mathrm{c}} - X_{\mathrm{w,res}}}{X_{\mathrm{o}} - X_{\mathrm{w,res}}} \tag{8}$$

where XC is the thickness of the charred sample, $X_{\mathrm{w,res}}$ is the thickness of the residue after the char was removed and X_0 is the original thickness of the sample.

Char yield or char to wood ratio is defined as

$$Y_{\mathrm{c}} = \frac{m_{\mathrm{c}} - m_{\mathrm{w,res}}}{m_{\mathrm{o}} - m_{\mathrm{w,res}}} \tag{9}$$

where m_{c} is the mass of the residue including the char, $m_{\mathrm{w,res}}$ is the mass of the residue without the char and m_0 is the original mass of the sample.

Char density is defined as

$$\rho_{\mathrm{c}} = \frac{m_{\mathrm{c}} - m_{\mathrm{w,res}}}{A(X_{\mathrm{c}} - X_{\mathrm{w,res}})} \tag{10}$$

where *A is* the area of the sample.

The measured properties related to charring are given in Table 5. Apparently, f_{c} increases with flux, the effect of flux on char yield is not pronounced and char density seems to be independent of flux.

The char contraction factor is related to char yield in the following manner

$$f_{\mathrm{c}} = Y_{\mathrm{c}}\left(\frac{\rho_{\mathrm{w}}}{\rho_{\mathrm{c}}}\right) \tag{11}$$

Because char density is independent of flux, f_{c} should be proportional to Y_{c}. However, the measured Y_{c} was not as strongly dependent on flux as f_{c}. We cannot account for this inconsistency but would point out some sources of experimental error in measuring and calculating these quantities. The calculation of f_{c} and Y_{c} (Eqns (8) and (9)) assumes that the char front was sharp and no pyrolysis

Table 5. Char properties

Species	Flux (kW m $^{-2}$)	f_c	Char yield Y_c	Apparent ρ_c (kg m $^{-3}$)
Redwood	17.8	0.523	0.27	181
	17.7	0.512	0.27	174
	25.8	0.563	0.26	168
	26.2	—	—	—
	38.5	0.613	0.27	183
	38.7	0.634	0.28	180
	53.6	0.835	0.32	156
	56.3	0.747	0.31	191
Southern pine	17.4	0.475	0.20	272
	17.4	0.456	0.24	287
	25.2	0.530	0.30	287
	26.9	0.469	0.20	294
	38.5	0.479	0.25	358
	38.6	0.444	0.23	355
	55.5	0.616	0.25	256
	56.0	0.583	0.26	312
Red oak	17.8	0.547	0.25	327
	18.7	0.567	0.26	328
	25.0	0.559	0.24	317
	25.8	0.564	0.25	333
	37.8	0.625	0.25	360
	38.4	0.606	0.25	345
	53.1	0.753	0.27	256
	53.6	0.705	0.31	312
Basswood	17.6	0.428	0.24	264
	17.8	0.408	0.22	251
	27.7	0.421	0.23	288
	25.5	0.430	0.22	260
	38.1	0.450	0.23	255
	38.7	0.409	0.20	227
	51.6	0.519	—	—
	53.4	0.523	0.23	239

occurred ahead of the char front. Char density calculation (Eqn (10)) assumes a volume of char based on a perfectly flat char front. In reality, the char front was preceded by a pyrolysis zone of approximately 10 mm. For this sample size, edge effects were also significant. Burning and charring occurred around the sample edges, resulting in convex residual wood sections. Because of the edge effects, some inaccuracy of the data is expected. However, measurement of f_c is more reliable than that of Y_c and p_c because it is based on direct measurement of the char thickness. Therefore, char contraction factor apparently increases with flux. The effect of flux on char yield and density remains unsolved.

DISCUSSION

The data presented so far are useful for future development of models to predict burning characteristics of wood. Although the factorial experimental design lends itself to further statistical analysis to elucidate the effects of material properties (Table 1), this report deals mainly with evident physical relationships between the measurable quantities.

We will discuss the relationships between heat release, mass loss and charring rates of wood. Heat release and mass loss rates are related by the effective heat of combustion as follows:

$$H_c = \frac{\mathrm{HRR}}{\dot{m}''} \tag{12}$$

Ignoring mass loss in advance of the char front and assuming the mass of char is negligible, average charring rate can be calculated from mass loss rate as follows:

$$\dot{c} = \frac{\dot{m}''}{\rho_w} \tag{13}$$

It follows that if HRR and H_c of a wood material are known, one can calculate average mass loss rate $\dot{m}''$ by Eqn (12) and subsequently average charring rate $\dot{c}$ (Eqn(13)).

Several factors complicate the modeling of wood combustion:

(1) Wood is a very diverse material. There is a great deal of variability between and within wood species, not to mention composites. Many physical and chemical properties are required to model burning characteristics of wood. Also, not all these properties are readily obtained or available in the literature.
(2) Models based on chemical properties such as major components of wood are gross approximations. As shown by Tran,[3] even within the hardwoods, which have similar lignin and carbohydrate fractions and very low extractive content, HRR varies a great deal, but seems to he independent of density (the most important physical property in wood).
(3) Moisture content significantly affects burning rate. A difference in moisture content of 10% results in a change of 20–30% in burning rate.[3, 11] Most existing models do not track moisture movement.
(4) Many other external factors such as the boundary conditions also affect burning rate. When wood of finite thickness is burned in heat release calorimeters, HRR increases toward the end of the test as a result of near adiabatic conditions of the unexposed side. The model must take into account the effects of the boundary conditions.

Therefore, sometimes analysis must be based on experimental data. The HRR data are quite readily obtained using state-of-the-art calorimeters. The following is an example of how mass loss and charring rates can be derived from HRR data.

First, an algorithm to estimate effective $H_{c,dry}$ is needed. It appears that $H_{c,dry}$ depends on material and heat flux (Fig. 11). Various correlation methods can be tried to fit the data to some properties of wood. However, there is no sound chemical or physical basis for such an analysis. Given the lack of a theoretically derived method, we employ an empirical correlation derived by Tran[3] for an average of a range of different wood materials:

$$H_{c,\mathrm{dry}} = 0.057\dot{q}''_e + 11.88 \tag{14}$$

with an R^2 value of about 0.6. The best linear regression fit through the data in Fig. 11 yields a similar equation with an R^2 value of 0.34 as a result of the wider scatter in this data set.

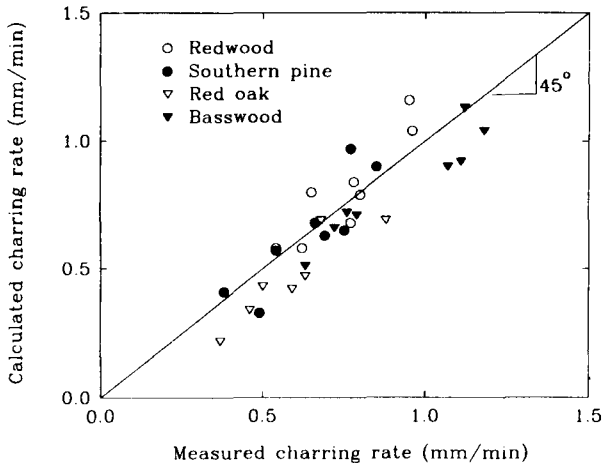

Figure 12. Calculated charring rate ($\dot{c}$) based on HRR compared to measured values.

The measured average heat release rates of all tests were used to calculate dry mass loss rate (Eqn (12)) using calculated $H_{c,dry}$ (Eqn (14)). Charring rates were then calculated using Eqn (13) and density of oven-dry wood. The calculated, $\dot{c}$ values were then compared with the measured values (Fig. 12). Agreement for all species and tests was quite good using this procedure despite a rough estimate of $H_{c,dry}$ and assumptions inherent in Eqn (13).

In theoretical modeling of wood combustion, surface recession is important. In the model of Parker, [12] surface recession is assumed to be due to contraction of the wood as it is converted to char. In the model of Fredlund,[19] char oxidation is the assumed mechanism for surface recession. As noted by White,[6,7] the char contraction factors found for ASTM E 119 exposures are consistent with values obtained by pyrolysis in a nitrogen environment, These values are also consistent with the values for the 50-kW m^{-2} exposure. Results in the study reported here suggest that, in addition to char contraction, oxidation eroded the char thickness. Char oxidation seemed to be most significant at low flux levels where the flow of pyrolyzate was significantly low and flaming combustion was confined to the large fissures in the char, allowing oxygen to reach the char surface elsewhere. At the highest flux level of 50 kW m^{-2}, where flaming combustion covered the char surface, air was excluded from the surface, resulting in essentially no char oxidation, as in the case of nitrogen atmosphere.

If the additional surface recession is due to oxidation, char yield should be less at the low flux levels, The char yield data showed this trend (Table 5). However, the scatter in the data was too great to support a definite conclusion.

CONCLUSIONS

The data presented in this paper are useful for further development and validation of models that deal with burning characteristics of wood. The database is limited to four species and does not include effects of moisture content or oxygen availability in ambient atmosphere.

Our results showed that heat release rate (HRR) is the most useful measurement because it is readily measured in oxygen consumption calorimeters. It also allows the calculation of mass loss and charring rates for wood materials. Only two parameters need to be known: effective heat of combustion and density. Heat of combustion and mass loss rate data are measured with advanced calorimeters such as the Cone Calorimeter or the calorimeter used in this study. Charring rate measurement is not a part of standard calorimetry. Therefore, HRR or mass loss rate can be used to characterize burning rate and to derive the charring rate of wood. The calculation procedures may also be applicable to composite materials that mainly consist of wood as combustibles, such as particleboard and flakeboard.

Although somewhat inconclusive, the data suggest that an algorithm for the surface recession associated with wood charring should include both char contraction and char oxidation. Char oxidation is a significant factor at significantly low heat fluxes, when the outflow of pyrolysis gases does not prevent sufficient oxygen from reaching the surface.

Authors' note

REFERENCES

1. J. J. Brenden, *Res. Pap. 217*, US Department of Agriculture, Forest Service, Forest Products Laboratory, Madison, WI (1973).
2. D. L. Chamberlain, *NBSIR* 82-2597, National Bureau of Standards, Gaithersburg, MD (1983).
3. H. Tran, Experimental heat release rate of wood products. In *Heat Release Rate in Fires*, ed. by V. Babrauskas and S. Grayson (in press).
4. ASTM, *Test Method E 1354-90*, American Society for Testing and Materials, Philadelphia, PA (1990).
5. ASTM, *Test Method E 90683*, American Society for Testing and Materials, Philadelphia, PA (1985).
6. R. H. White, *Charring Rates of Different Wood Species*, PhD dissertation, University of Wisconsin, Madison, WI (1988).
7. R. H. White, and E. V. Nordheim, *Fire Technol.* **28**(1), 5 (February 1992).
8. ASTM, *Test Method E 119-83*, American Society for Testing and Materials, Philadelphia, PA (1985).
9. E. L. Schaffer, *Res. Pap. FPL 69*, US Department of Agriculture, Forest Service, Forest Products Laboratory, Madison, WI (1967).
10. S. Hadvig, *Charring of Wood in Building Fires*, Technical University of Denmark, Lyngby, Denmark (1981).
11. E. Mikkola, *Res. Rep. 689*, Technical Research Center of Finland.
12. W. Parker, *Prediction of Heat Release Rate of Wood*, PhD

dissertation, George Washington University, Washington, DC (1988).
13. H. Tran, *Proceedings, Heat and Mass Transfer in Fires*, HTD Vol. 141, The American Society of Mechanical Engineers, United Engineering Center, New York (1990).
14. R. H. White and E. L. Schaffer, *Fire Technol.* **14**(4), 279 (1978).
15. J. Quintiere and M. Harkleroad, *NBSIR 84-2943*, National Institute of Standards and Technology (1984).
16. M. Janssens, *Proceedings, International Conference on Fires in Buildings*, Techtomic, Lancaster, PA (1989).
17. *Wood Handbook*, Chapter 3, US Dept Agric., Agric. Handbook 72 (1987).
18. R. H. White and E. L. Schaffer, *Wood and Fiber* **13**(1), 17 (1981).
19. B. Fredlund, *A Computer Program for the Analysis of Timber Structures Exposed to Fire*, Lund Institute of Technology, Lund, Sweden (1985).